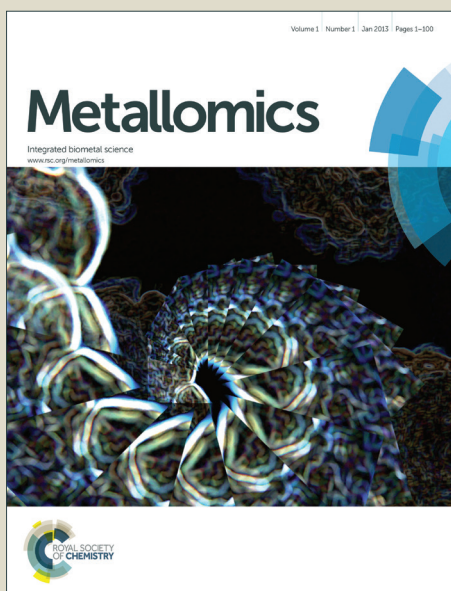


Metallomics

Accepted Manuscript



This is an *Accepted Manuscript*, which has been through the Royal Society of Chemistry peer review process and has been accepted for publication.

Accepted Manuscripts are published online shortly after acceptance, before technical editing, formatting and proof reading. Using this free service, authors can make their results available to the community, in citable form, before we publish the edited article. We will replace this *Accepted Manuscript* with the edited and formatted *Advance Article* as soon as it is available.

You can find more information about *Accepted Manuscripts* in the [Information for Authors](#).

Please note that technical editing may introduce minor changes to the text and/or graphics, which may alter content. The journal's standard [Terms & Conditions](#) and the [Ethical guidelines](#) still apply. In no event shall the Royal Society of Chemistry be held responsible for any errors or omissions in this *Accepted Manuscript* or any consequences arising from the use of any information it contains.

Distribution and speciation of bromine in mammalian tissue and fluids by X-ray fluorescence imaging and X-ray absorption spectroscopy

Melanie J. Ceko,^a Katja Hummitzsch,^b Nicholas Hatzirodos,^b Wendy Bonner,^b Simon A. James,^c Jason K. Kirby,^d Raymond J Rodgers,^b and Hugh H. Harris^a
DOI: 10.1039/b000000x [DO NOT ALTER/DELETE THIS TEXT]

Bromine is one of the most abundant and ubiquitous trace elements in the biosphere and until recently had not been shown to perform any essential biological function in animals. A recent study demonstrated that bromine is required as a cofactor for peroxidase-catalysed formation of sulfilimine crosslinks in *Drosophila*. In addition, bromine dietary deficiency is lethal in *Drosophila*, whereas bromine replenishment restores viability. The aim of this study was to examine the distribution and speciation of bromine in mammalian tissues and fluids to provide further insights into the role and function of this element in biological systems. In this study we used X-ray Fluorescence (XRF) imaging and Inductively Coupled Plasma – Mass Spectrometry (ICP-MS) to examine the distribution of bromine in bovine ovarian tissue samples, follicular fluid and aortic serum, as well as human whole blood and serum and X-ray Absorption Spectroscopy (XAS) to identify the chemical species of bromine in a range of mammalian tissue (bovine, ovine, porcine and murine), whole blood and serum samples (bovine, ovine, porcine, murine and human), and marine samples (salmon (*Salmo salar*), kingfish (*Seriola lalandi*) and *Scleractinian coral*). Bromine was found to be widely distributed across all tissues and fluids examined. Statistical comparison of the near-edge region of the X-ray absorption spectra with a library of bromine standards led to the conclusion that the major form of bromine in all samples analysed was bromide.

Introduction

Bromine (Br) is one of the most abundant and ubiquitous trace elements in the biosphere and until recently had not been shown to perform any essential function in plants, microorganisms, or animals.^{1, 2} Between 1970 and 1984, it was suggested that bromine, along with ten other elements, should be added to the list of essential ultratrace elements which had previously only included chromium, molybdenum and selenium.³ By the end of this 14-year period, only weak evidence existed to support the view that bromine is essential, with one of the key findings being that bromide ($\text{Br}^-_{(\text{aq})}$) can substitute for part of the chloride (Cl^-) requirement for chicks. In particular, dietary supplementation (676-1352 mg/kg) counteracted most of the symptoms of Cl^- deficiency in chicks fed a Cl^- deficient diet.⁴ In 1990, one additional study reported that, when compared to goats fed 20 mg bromine/kg diet, goats fed a 0.8 mg bromine/kg diet exhibited depressed growth, fertility, reduced life expectancy and more abortions.⁵ Microscopic examination of tissues and organs of bromine deficient goats has shown abnormalities in tissue sections of the thyroid, heart, lungs, pancreas and ovaries.⁶ These findings provide little insight into a possible biochemical role for this element, beyond indicating that it may serve as an electrolyte.³ This led to the general assumption that the biological behaviour of bromine is similar to chlorine in that the administration of $\text{Br}^-_{(\text{aq})}$ results in some displacement of body Cl^- , and vice versa.⁷ This assumption has however been found to be invalid for the thyroid gland. In studies on the interaction of bromine with iodine in the rat thyroid under the conditions of enhanced $\text{Br}^-_{(\text{aq})}$ intake, Pavelka *et al.* found that contrary to other tissues, $\text{Br}^-_{(\text{aq})}$ replaced iodide (I^-) as opposed to Cl^- .^{8, 9} A recent study demonstrated that bromine is required as a cofactor for peroxidase-catalysed formation of sulfilimine crosslinks in *Drosophila*. Bromine dietary deficiency led to physiologic dysfunction in *Drosophila*, while repletion of this trace element reversed the dysfunction.²

Biological activity of brominated species

The potential biological roles of brominated species in biological organisms are still to be fully elucidated. Hawkins *et al.* (2001) conducted an experiment to show that hypochlorous acid (HOCl) and hypobromous acid (HOBr) react with different selectivity with cellular targets, and that the resultant radical formation may result in cell lysis.¹⁰ With regard to the original generation of HOBr, they articulate that myeloperoxidase can catalyse the reaction of hydrogen peroxide with $\text{Br}^-_{(\text{aq})}$. However, under physiological conditions Cl^- is the preferred substrate. This is not the case for eosinophil peroxidase which preferentially generates HOBr.¹¹ The reactivity of HOBr with biological molecules is less well

characterised but amino acids and proteins appear to be major targets, with the species reacting with fatty acid side chains and lipid-soluble antioxidants to a much greater extent than HOCl.¹²⁻¹⁴ This species has also been reported to induce red blood cell lysis approximately 10 times more rapidly than HOCl.¹⁰ In a later study to ascertain the rate constants for reactions of HOBr with protein components, most residues reacted 30-100 fold faster with this species than with the Cl⁻ containing acid.¹² More recently, the contribution of HOBr to optimal and efficient microbial killing has been recognised as essential.¹⁵

Marcinkiewicz *et al.* (2005) investigated the role of another brominating oxidant, taurine bromamine, and found that this species exerted strong bactericidal effects on *E. coli*.¹⁶ They surmised that bromination pathways may be physiologically relevant given that they still operate even when the Cl⁻ concentrations are 1000 to 10 000 times higher than Br⁻_(aq) concentrations. Maines *et al.* (2006) investigated the cytotoxic effects of activated bromine on human fetal osteoblasts in vitro and showed that sodium bromide (NaBr) is more cytotoxic than either sodium hypochlorite or activated sodium hypobromite.¹⁷ Thus, it appears that there are a range of chemical modifications induced by Br⁻_(aq) based species which are still not completely understood. As part of the study which demonstrated the essentiality of Br to *Drosophila*, the authors showed that bromine is an essential trace element for assembly of collagen IV scaffolds in tissue development and architecture.² More specifically, McCall *et al.* (2014) established that Br⁻_(aq) converted to HOBr is required for sulfilimine formation within collagen IV.

Bromine in nature and from anthropogenic sources

In nature bromine is found mostly as Br⁻; bound to metals in the form of inorganic salts.¹⁸ The main natural source of Br⁻_(aq) is in the sea where the average concentration of 65-71 mg/L is several orders of magnitude larger than in freshwater systems.¹⁹ In natural soils the common range for bromine mass fractions varies from 5 to 40 mg/kg.²⁰ Bromine occurs naturally in food for humans and feed for animals.¹⁹

The three major contributors to manmade release of bromine into the environment are: mining; industrial emissions e.g. 1,2-dibromomethane (a scavenger in leaded fuel); and from the use of fertilisers and pesticides in agriculture where brominated hydrocarbons such as methyl bromide are employed for pre-planting fumigation of soils and post-harvest fumigation of agricultural products.¹⁹ These processes can significantly increase the concentration of bromine in the environment.

Chemical disinfectants, such as those used to reduce concentrations of microorganisms in potable water, react with natural organic matter, Br⁻_(aq), and iodide, to form complex mixtures of potentially toxic disinfection by-products. The types and concentrations of the by-products formed during disinfection vary depending on factors such as source water conditions, disinfectant type (e.g. chlorine, ozone, chloramine), and treatment conditions.²¹ It is worth noting that although strict regulations exist in developed countries for the maximum threshold of certain bromine-based disinfection by-products, Br⁻_(aq), specifically, is not regulated.²²

Finally, polybrominated diphenyl ethers (PBDEs) are used as flame retardants in plastics and in textile coatings with commercial products consisting predominantly of penta-, octa-, and decabromodiphenyl ether mixtures. PBDEs can be bioaccumulated and biomagnified in the environment, and comparatively high concentrations are often found in terrestrial (e.g. through application of biosolids) and aquatic biotopes from different parts of the world.²³⁻²⁵

Bromine toxicity in mammalian systems

With such prevalent exposure to bromine, coming from natural and anthropogenic sources, it is not surprising that numerous studies have been conducted into the impact of chronic bromine exposure on mammalian systems. In 1985, Owens *et al.* showed that bromine can be extremely harmful to organisms. In a tracer experiment involving the widespread application of potassium bromide to a field plot (16.8g/m²), 25 adult beef cows were allowed to graze on the test area two weeks after the Br⁻_(aq) application.²⁶ Three days later 19 of the animals had died, highlighting the need for an evaluation of the toxicity of the Br⁻_(aq) ion.¹⁹ Throughout the 1980s several authors confirmed that large doses of Br⁻_(aq) could reduce fertility, impact the rate of survival of offspring, and result in reduced production of thyroxine because the excess Br⁻_(aq) competes with I⁻ in the synthesis of this hormone.^{27, 28} In 1993, Flury *et al.* suggested that chronic bromine toxicity affects mainly the endocrine and reproductive systems of mammals and Pavelka *et al.* further suggested that high Br⁻_(aq) levels can influence iodine metabolism by either decreasing the iodine accumulation in the thyroid and skin and/or by increasing the excretion of iodine by the kidneys.¹⁸ More recent studies have focused less on Br⁻_(aq) and more on the potential toxicology of brominated disinfection by-products. Several authors focusing on dibromoacetic acid have concluded that chronic exposure to even low levels of this chemical (1 mg/kg body weight per day) adversely affects reproductive function in male rabbits, and delays pubertal development and compromises sperm quality in rats.²⁹⁻³¹

Speciation of bromine in terrestrial and mammalian systems

Synchrotron X-ray fluorescence imaging and X-ray absorption spectroscopy (XAS) are ideal techniques for investigating the chemical speciation and distribution of elements heavier than silicon in biological systems, with minimal sample preparation required.³² The lack of sample preparation means that XAS has the distinct advantage that it reports all chemical forms of an element present within a sample, compared to other methods which may report only extractable or soluble forms. X-ray absorption spectra of a number of organic bromine compounds of biological relevance have been measured previously.³³ Although Feiters *et al.* (2005) selected model compounds with the specific metabolism of brown algae in mind, the relevance of their data to any biological X-ray absorption studies at the bromine K edge, is unquestionable. More specifically their model compounds depict the most probable chemical environments bromine would be found in, with the most distinctive spectrum being that of NaBr. While there are no previous reports of bromine K-edge XAS conducted on mammalian systems, Leri *et al.* (2012) have recently shown that the X-ray absorption spectra of several bromine containing isolated humic materials and organic-rich surface soil profiles are sufficiently different to allow the identification of species within these terrestrial matrices. These recent XAS studies have dramatically changed the view of bromine in the environment to a more complex system that involves biogeochemical cycling between inorganic and organic species as opposed to being an unreactive inorganic species.³⁴

Herein we investigate the distribution of bromine in bovine ovarian sections using X-ray fluorescence (XRF) imaging and validate the observed widespread distribution of this element in bovine and human biological fluids using Inductively Coupled Plasma – Mass Spectrometry (ICP-MS). X-ray Absorption Near-Edge Structure (XANES) spectroscopy is then employed to investigate the speciation of bromine in a range of mammalian (bovine, ovine, porcine, murine and human) ovary, liver, whole blood, and serum samples. The main rationale for selecting bovine ovarian tissue included: it is a highly structured organ crucial to female reproduction; there are extensive structural and physiological similarities between the adult bovine ovary and the human ovary; and the potential for chronic bromine toxicity to adversely affect the endocrine and reproductive systems of mammals. The demonstration that bromine exists in different forms in different tissues by XANES would indicate that its presence is more than simply adventitious.

Experimental

Sample collection and preparation for XRF imaging

Bovine ovaries were collected from T&R Pastoral's abattoir, Murray Bridge, South Australia. Ovaries were collected in pairs from non-pregnant heifers (n=19) and transferred into ice-cold Hank's balanced-salt solution (which contained no bromine) and transported on ice (~0°C for 2 h) to the laboratory. Sections for XRF imaging were selected on the grounds that they contained a mix of anatomical structures; chosen specimens (n = 45, selected from the 19 pairs of ovaries above) were then frozen in O.C.T. compound (ProSciTech, Thuringowa, QLD, Australia - which contained no bromine) and stored at -80°C until sectioning.

Ovaries were sectioned at a thickness of 30 µm for XRF imaging with an adjacent 6 µm section taken for haematoxylin and eosin (H&E) staining to subsequently align with XRF data. Sectioning was performed on a CM1800 Leica cryostat (Adeal Pty Ltd., Altona North, Vic, Australia). Sections for XRF analysis were supported on Ultralene thin film affixed to a 24 x 36 mm photographic slide frame. Sections were transferred from the cryostat to the thin film using a combination of stainless steel tweezers and an artist grade Filbert type synthetic paint brush with care being taken to only contact frozen O.C.T. compound. Tissues were then desiccated under vacuum overnight (1-2 kPa) and then stored in a desiccator at atmospheric pressure until analysis.

Sample collection and preparation for total element analysis

Total Br, Cu, Fe, Se and Zn concentrations in bovine ovaries follicular fluid, bovine serum, human whole blood and serum were determined using microwave-assisted acid digestion and ICP-MS analysis procedures.

For the follicular fluid samples, bovine ovaries were collected from a local abattoir as described previously and the follicular fluid of the largest healthy follicles individually extracted with a sterile needle and syringe (n = 29). Approximately 0.7 g of follicular fluid was transferred into 1.5 mL microcentrifuge tubes and frozen at -80°C.

Aortic whole blood from non-pregnant heifers (n = 12) were collected at the abattoir using sterile needle and syringes, transferred into 15 mL centrifuge tubes and transported on ice (~3hr) to the laboratory. In the laboratory, samples were centrifuged for 15 min at 1500 g, with the resultant serum (~1 g) being aliquoted in triplicate, into 5 mL centrifuge vials. The bovine serum samples were stored at -20°C until digestion and analysis.

Human whole blood samples were taken from one male (40 years old, healthy) and one female patient (30 years old,

healthy) in the Discipline of Pharmacology, The University of Adelaide, SA and dispensed into four weighed heparin containing 9 mL centrifuge tubes. The samples were allowed to settle upright at room temperature for 30 min before one tube for each patient was aliquoted into three 5 mL plastic vials (~ 2 g per vial) and placed on dry ice. The frozen samples were weighed and stored at -80 °C until digestion and analysis. Serum from human whole blood were collected following 30 min settling at room temperature, the remaining three whole blood samples for each patient were centrifuged for 15 min at 2000 g at 22 °C and the separated serum pipetted into three weighed 5 mL vials (~ 1 g per vial). The samples were weighed and stored at -80 °C until digestion and analysis.

Sample collection and preparation for XAS analysis

Bovine, porcine, ovine and murine ovary and liver samples were collected for XAS analysis. Bovine (n = 3) domestic cattle and ovine (n = 3) domestic sheep samples were collected from T&R Pastoral's abattoir, Murray Bridge, South Australia; porcine (n = 3) pig samples from Menzel's Meats Pty Ltd., Kapanda, South Australia; and murine (n = 4) mice samples from Professor Kennaway, The University of Adelaide, South Australia. The liver was additionally analysed given the suite of biological functions it performs and the possibility that bromine may be associated with this organ's detoxification processes. For all species, representative 4 mm³ tissue sections were dissected from each organ, stored in quadruplicate in 5 mL specimen containers and frozen at -80 °C until XAS analysis. Two marine fish samples: *Salmo salar* and *Seriola lalandi* (sourced from a local restaurant), and one coral sample (SA Museum sample code H382 *Scleractinian coral*) were also included to provide a comparison with the marine environment, where bromine concentrations are far higher than in the terrestrial one.

Aortic whole blood was sourced from the same four species (bovine, ovine, porcine and murine) and collected into heparin-containing tubes and initially stored on wet ice for 2-3 h. Half the blood volume was then aliquoted into 5 mL tubes and frozen on dry ice. The remaining aliquot was centrifuged for 15 min at 4000 rpm, the resultant serum aliquoted into 5 mL tubes and frozen on dry ice. All blood samples were then stored at -80 °C until XAS analysis.

Preparation of standard solutions for XAS

Eleven bromine standards as displayed in Table 1 were selected for their chemically distinct forms and purchased from Sigma Aldrich (Castle Hill, NSW, Australia) at the highest available analytical grade. The standards were dissolved or solubilised for analysis by XAS. Water-soluble solids were pre-weighed into 12 mL glass vials and 10 mL ultrapure deionised water (Milli-Q, Millipore) added just prior to analysis (final concentration 2 mM). Water insoluble species were solubilised using a micellar sodium dodecyl sulfate (SDS) (16.2 mM) solution, into which a methanol or DMSO stock solution of the compound was dispersed (Table 1). All solutions were carefully inverted several times to homogenise the solutions, but in the case of SDS dispersed standards, vigorous inversion was avoided to prevent bubble formation.

Table 1: Summary of bromine standards analysed by XAS

Standard	Solubility
Sodium bromate	Water
Sodium bromide	Water
Dibromoacetic acid	Water
2-bromohexadecanoic acid	Methanol/SDS
Tralomethrin	DMSO/SDS
Bromodichloromethane	Water
Bromochloroacetic acid	Water
Bromoacetonitrile	Water
Decabromodiphenyl ether	DMSO/SDS
3,3',5,5'-tetrabromobisphenol A	Methanol/SDS
3-bromodiphenyl ether	DMSO/SDS

Instrumentation and operating conditions

X-ray fluorescence imaging (XRF)

The distribution of elements (i.e. Br, Fe, and Zn) throughout selected 30 μm bovine ovarian sections was mapped at the XFM beamline at the Australian Synchrotron, Clayton, Victoria, Australia. An incident beam of 15.75 keV X-rays was chosen to induce K-shell ionization of elements with atomic numbers below 37 ($Z \leq \text{Rb}$), while providing adequate separation of the Rayleigh and Compton peaks from the elemental fluorescence of interest, i.e. bromine (see Fig. S1). The incident beam was focused to a $\sim 2 \mu\text{m}$ spot for all scans (full-width at half maximum) using a Kirkpatrick-Baez mirror pair and specimens were fly-scanned through the X-ray focus with either a 2 (fine scans) or a 6 μm (coarse scans) vertical step size. The resulting XRF was collected in event-mode using the low-latency, 384-channel Maia XRF detector (positioned in the backscatter geometry) and the full XRF spectra were used to reconstruct elemental maps of the specimen using a virtual pixel size of 2 or 6 μm (fine and coarse scans, respectively). The effective per pixel dwell times for the fine and coarse scans were 7.81 ms or 2.44 ms, respectively and the largest scan depicted in this study was 1291×1579 pixels in size. Single element foils of Mn and Pt (Micromatter, Canada), were scanned in the same geometry and used as references to establish elemental quantitation. Deconvolution of the Maia data was performed using the GeoPIXE v6.5g (CSIRO, Australia) that incorporates a linear transformation matrix to perform spectral deconvolution.³⁵ Spectra were calibrated using the metal foil measurements, and corrections made for self-absorption in the sample, absorption in air, and the efficiency response of the detector.³⁶ The detected X-ray photons from each pixel were related to calculated-model fluorescence X-ray yields for an assumed specimen composition and thickness. The composition and thickness of the Ultralene film was known from the manufacturer's specifications and the composition and average density typical of dried organic material ($\text{C}_{22}\text{H}_{10}\text{N}_2\text{O}_4$ and 1.42 g cm^{-3} respectively), was used to model the tissue. Absorption effects for XRF from the lowest atomic number element relevant to this study (Ca $K\alpha$) were negligible for this specimen type.

Total element concentrations in human and bovine samples

Total concentrations of Br, Cu, Fe, Se, and Zn in human and bovine samples were determined using a modified US EPA 3052 method with strong acid microwave-assisted digestion and ICP-MS analysis.

Frozen pre-weighed aliquots of human whole blood (1.6 – 2.5 g) ($n=6$), human and bovine serum (1.1 – 1.7 g) ($n=6$ and 12, respectively), and bovine follicular fluid (0.26 – 1.1 g) ($n=29$) were digested and analysed at CSIRO's Land and Water Flagship Laboratory, Waite Campus, Glen Osmond, South Australia. The samples were cold digested overnight in 7 mL of concentrated nitric acid (Fisher Scientific, AR Grade, 70%) and 3 mL of concentrated hydrogen peroxide (Chem Supply, AR Grade, 30%). The samples were then subjected to a closed vessel microwave-assisted digestion procedure in a CEM MARS express oven using the following time and temperature program: 50 min ramp to 180°C and then held constant at 180°C for 55 min. Following cooling, the digest solutions were diluted to 50 mL with ultrapure deionised water (Milli-Q, Millipore), filtered through 0.45 μm syringe filters (Sartorius) and analysed for total Br, Cu, Fe, Se, and Zn concentrations by ICP-MS (Agilent 7500ce).

Total Br, Cu, Fe, and Zn concentrations in digest solutions were determined using m/z 79, 63 57, and m/z 66, respectively in collision cell mode with helium gas at 4 ml min^{-1} . Selenium concentrations were determined using m/z 78 in reaction mode with hydrogen gas at a flow rate of 4 ml min^{-1} . Sample digests were analysed using a 0.4 ml/min micromist nebuliser and Peltier-cooled quartz Scott's type double pass spray chamber. The ICP-MS instrument was optimised daily to minimise double charged and oxide interferences to $< 2\%$ (m/z 70/ m/z 140) and $< 1\%$ (m/z 156/ m/z 140), respectively.

The standard reference materials, NIST 1568b Rice Flour and NIST 1577b Bovine Liver, were used for quality control purposes to determine the accuracy of the digestion and analysis procedures. The recoveries of all elements analysed were in close agreement with certified values for NIST 1568b and both the certified values and non-certified Br value for NIST 1577b (Table 1). An additional quality control check occurred by spiking selected samples with $50 \mu\text{g Br L}^{-1}$ that resulted in Br recoveries of $98 \pm 3\%$. Precision was assessed by analysing duplicates of selected samples with RSD for all elements analysed of $< 4.2\%$.

Table 1: Comparison of total elemental analysis (mean±SD) in standard reference materials NIST 1568b Rice Flour (n=6) and NIST 1577b Bovine Liver (n=4) against certified values.

Element	NIST 1568b Rice Flour		NIST 1577b Bovine Liver	
	Certified Value	Found Value	Certified Value	Found Value
	$\mu\text{g g}^{-1}$	$\mu\text{g g}^{-1}$	$\mu\text{g g}^{-1}$	$\mu\text{g g}^{-1}$
Bromine	8.31 ± 0.61	8.31 ± 0.35	9.7 ^A	9.8 ± 0.4
Copper	2.35 ± 0.16	2.31 ± 0.07	160 ± 8	158 ± 6
Iron	7.42 ± 0.44	7.34 ± 0.34	184 ± 15	173 ± 2
Selenium	0.365 ± 0.029	0.353 ± 0.01	0.73 ± 0.06	0.71 ± 0.02
Zinc	19.42 ± 0.26	19.98 ± 0.30	127 ± 16	125 ± 3

^A Non-certified value

Assessment of statistical significance

Statistical significance was assessed by conducting an ANOVA across the four groups follicular fluid, aortic serum, human whole blood, human serum, followed by application of a post hoc t-test (two sample assuming equal variances).

X-ray Absorption Spectroscopy (XAS)

Bromine K-edge X-ray absorption spectra of the dissected frozen hydrated tissues (ovary and liver) or 50 μL aliquots of whole blood or serum for each mammalian species were recorded on the XAS beamline at the Australian Synchrotron, Clayton Victoria, Australia. Samples were secured using kapton tape in polymethylmethacrylate cells, and maintained at 77K in liquid nitrogen before loading into a Cryo Industries (Manchester, NH, USA) cryostat for analysis, where they were maintained at ~ 5 K during data collection. The Br K-edge was monitored over repeat scans on the same sample position; a lack of variation of the spectrum indicated that photodamage was not evident under these conditions.

The X-ray beam was monochromated by diffraction from a pair of Si(111) crystals. Spectra were recorded in fluorescence mode on a 100-pixel Ge detector array at 90° to the incident beam. The energy ranges used for XANES data collection were as follows: pre-edge region, 13 272 – 13 452 eV (10 eV steps); XANES region, 13 452 – 13 522 eV (0.25 eV steps); post-edge region, 13 522 – 13 855 eV (0.1 \AA^{-1} steps in k space to $k = 7 \text{\AA}^{-1}$). The beamline energy was externally calibrated using the spectrum of a Se foil recorded in transmission mode. The first peak of the first derivative of this spectrum was assumed to be at 12 658 eV.

Data analysis, including calibration, averaging, and background subtraction of all spectra was performed using EXAFSPAK (G. N. George, Stanford Synchrotron Radiation Laboratory, Stanford, CA). Linear combination fits of XANES spectra were performed over the region 13.45–13.50 keV. Interpolation of data within the narrow XANES energy range 13.46 – 13.49 keV was carried out in OriginPro 7.5 and Principal Component Analysis (PCA) of the XANES spectra was carried out in The Unscrambler X 10.1.0.

Liquid chromatography-tandem mass spectrometry (LC-MS/MS) analysis

Liquid chromatography-mass spectrometry-mass spectrometry (LC-MS/MS) (TSQ Quantum, Thermo Finnigan) was performed at CSIRO's Land and Water Laboratory, Waite Campus, Glen Osmond, South Australia in order to validate the XANES fitting which suggested the bovine ovarian samples contained around 12% tetrabromobisphenol A (TBBPA). Approximately 2 g of wet mass ovarian tissue (sourced from five separate ovarian samples) was ground with anhydrous sodium sulfate and extracted with dichloromethane and hexane (3:1; 400 ml) for 16 h in a Soxhlet apparatus. The subsequent LC-MS/MS protocol was modified from that previously reported by Johnson-Restrepo *et al.* (2008)³⁷ and can be found in the Supplementary Material.

Results and discussion

Distribution of bromine in bovine ovarian tissue by XRF imaging

XFM was used to image key structural features and provide information on element distribution within different bovine ovarian cross sections. From a qualitative perspective several elemental distribution trends were identified for Br, Fe and Zn, with all ovaries showing a strong signal for these three elements (Figs. 1, 2 and S1). Bromine was widely distributed across all ovarian sections with higher concentrations apparent in what appears to be the sub-endothelial basal lamina of blood vessels and capillaries (Fig. 1B) and arterioles (Fig. 2B), in the smooth muscle cells, and in regions of comparatively higher total density as suggested by the Compton maps (see Figs. S2 and S3). In addition, elevated bromine (relative to the background tissue levels) was observed across all stromal compartments, and was often correlated with higher than background Zn levels. Based on the recent findings of McCall *et al.*², which state that bromine is essential for

the assembly of collagen IV scaffolds, in conjunction with the immunohistochemistry results of Rodgers *et al.*³⁸ and Irving-Rodgers *et al.*³⁹, one would expect to see higher bromine concentrations in the aforementioned regions based on this observable expression of collagen IV, in addition to the collagen IV rich basal laminae of follicles.

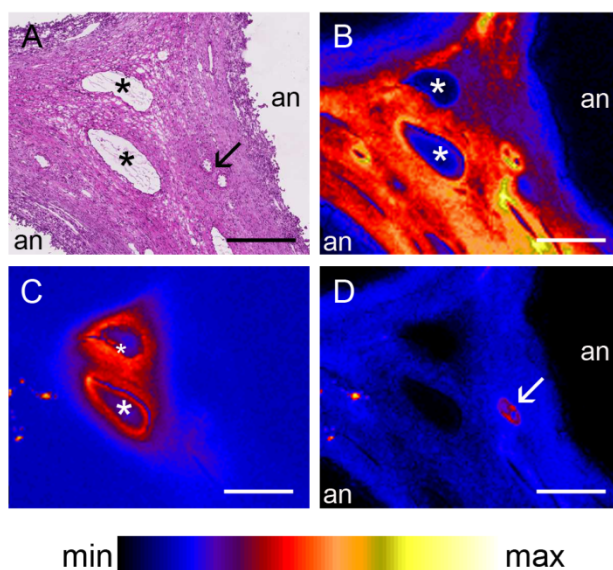


Figure 1: (A) H&E stained section of a bovine ovary containing portions of three small (< 4 mm) to small-medium (4-8 mm) follicles alongside Br (B), Fe (C) and Zn (D) elemental distribution maps generated by XRF imaging. Maximum pixel values for Br, Fe and Zn are 36.2 ppm, 506 ppm and 67.3 ppm, respectively. **an** represents antral cavity of follicle; * represents vessels; ↙ represents capillaries. Scale bar: 300 μm .

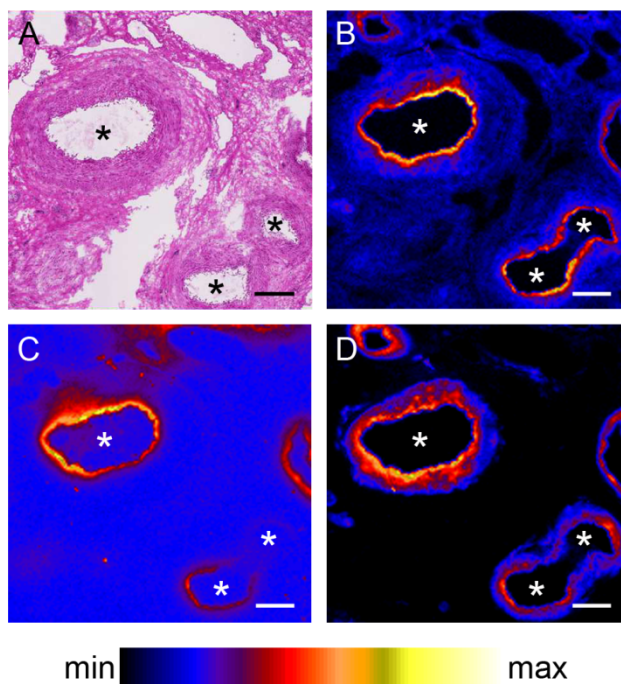


Figure 2: (A) H&E stained section of a bovine ovary containing arterioles alongside Br (B), Fe (C) and Zn (D) elemental distribution maps generated by XRF imaging. Maximum pixel values for Br, Fe and Zn are 24.7 ppm, 338 ppm and 56.7 ppm, respectively. * represents arterioles. Scale bar: 200 μm .

Elemental concentrations in human and bovine samples

The concentrations of Cu, Fe, Se and Zn in human (whole blood and serum) and bovine (serum and follicular fluid) samples using microwave-assisted acid digestion and ICP-MS analysis (Table 2) were similar to those determined by synchrotron-based XRF analysis.

The estimated mean mass fraction of bromine determined by analysis of XRF images of bovine follicle walls was $8.56 \mu\text{g g}^{-1}$ (SD = 6.30) compared with the total analysis bromine mass fraction for follicular fluid of $23.5 \mu\text{g g}^{-1}$ (SD = 3.8). This suggested that the follicular fluid contained within the antral cavities concentrated the bromine to a greater extent than in the surrounding tissue. However, we note that XRF analysis is subject to significant uncertainty mainly due to estimation of tissue section thickness/density, and selection bias from sampling small areas of interest yielding the evidently large standard deviation quoted above. Total bromine mass fractions from ICP-MS analysis in bovine serum were significantly higher ($p < 0.01$) than those in human serum (Table 2). Conversely, Se concentrations in bovine serum were significantly lower ($p < 0.01$) when compared with the human serum, which perhaps reflects distinct dietary intakes of this element. No significant differences were observed between the bovine and human fluids for the other trace elements analysed (Cu, Zn and Fe).

Table 2: Total elemental mass fractions ($\mu\text{g g}^{-1}$, mean \pm SD) for blood, serum and follicular fluid samples as determined by microwave-assisted acid digestion and ICP-MS analysis.

Element	Human male (n=3 from one individual)		Human female (n=3 from one individual)		Bovine	
	Whole blood	Serum	Whole blood	Serum	Serum (n=12)	Follicular fluid (n=29)
Bromine	8.0 ± 1.1	8.9 ± 0.9	10.3 ± 1.3	10.2 ± 1.2	30.7 ± 4.9	23.5 ± 3.8
Copper	0.83 ± 0.06	1.1 ± 0.1	0.70 ± 0.0	0.83 ± 0.06	1.2 ± 0.3	0.9 ± 0.2
Iron	500 ± 35	1.8 ± 0.2	450 ± 20	2.0 ± 0.1	1.7 ± 0.8	1.8 ± 1.0
Selenium	0.32 ± 0.05	0.3 ± 0.2	0.4 ± 0.2	0.4 ± 0.3	0.07 ± 0.02	0.05 ± 0.02
Zinc	5.2 ± 0.3	0.9 ± 0.2	5.1 ± 0.2	1.0 ± 0.1	1.0 ± 0.5	1.1 ± 0.5

According to the findings of Underwood *et al.* (1971) bromine occurs at naturally low concentrations of 3 - 4 mg/L in human serum; the values reported here for human and bovine serum are significantly higher.¹ The tenfold higher concentrations of bromine in bovine serum versus normal human serum concentrations raises some important questions regarding the dietary and environmental exposure to bromine for the cattle involved in this study.

Identification of bromine chemical form in mammalian tissues and fluids by XAS

Compilation of bromine standards

Figure 3 depicts the bromine K-edge XANES spectra of the eleven standards summarised in Table 1. Collection of these data enabled the compilation of a model compound library. This allowed quantitative comparisons to be made with the mammalian tissue (liver and ovary) and fluid (whole blood and serum) based spectra, with the ultimate aim being to deduce the speciation of bromine within these samples.

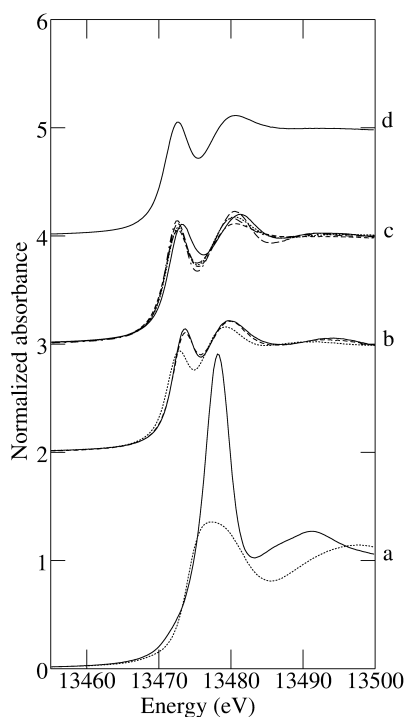


Figure 3: Library of Br K-edge X-ray absorption near edge spectra of organic and inorganic Br standards (2 mM solutions except where noted otherwise). a) sodium bromate (solid), sodium bromide (dotted). b) 3-bromodiphenyl ether (solid), 2-bromohexadecanoic acid (dotted), tetrabromobisphenol A (dashed). c) decabromodiphenyl ether (solid), bromochloroacetic acid (dotted), tralomethrin (dashed), bromodichloromethane (long dashed), bromoacetonitrile (dot dashed). d) dibromoacetic acid (solid).

Comparison of Figure 3 with the bromine standard library produced by Leri *et al.* (2012) supports their observation that the energy absorption maximum shifts to higher values with an increase in bromine oxidation state (e.g. potassium bromide at 13 477.3 eV to a bromate salt at 13 478.1 eV). Furthermore, organic bromine compounds give rise to sharp lower-energy peaks around 13,473 eV. Our model compound library supports the assertion by Feiters *et al.* (2005) that it is not possible to use the bromine K-edge spectra to easily classify brominated organic compounds as either aliphatic or aromatic on the basis of their bromine K-edge spectra.

Comparison of bromine XANES across species

Figure 4 compares the ovary, liver, blood and serum bromine XANES spectra for all mammalian species analysed, as well as the marine samples. The spectra have been grouped according to species to ascertain in the first instance whether there was a discernible difference between the bromine form within a species, and then to visually compare whether there were any obvious differences between species. The ovary was the first organ of interest given that high bromine had already been observed in the bovine ovaries through XRF imaging. The liver was additionally analysed given the suite of biological functions it performs and the possibility that bromine may be associated with any of these processes. On first inspection it would appear that all the spectra in Figure 4 are essentially identical, however the spectrum of the sodium bromide standard has a somewhat broader peak, implying that the mammalian spectra must either have a small contribution from at least one other bromine based species, or that the local environment surrounding bromide in the biological matrices is somehow different to the simple aqueous standard. One phenomenon which may account for this discrepancy is the nature of the halogen bonding occurring in the biological samples. More specifically, in the biological samples the potential interaction of polarisable Br with backbone carbonyls and/or carboxylate groups of amino acid residues would not be well emulated in the aqueous bromide standard. Additionally, the bromine in the biological samples may be halogen bonding to amide groups which would not be represented in the $\text{NaBr}_{(\text{aq})}$ standard. Given that bromide is a very weak base, the pH of the freshly prepared bromide model solution would be expected to be neutral, hence pH

variation is unlikely to be the source of discrepancy between the model solution and the frozen-hydrated tissue samples. Interestingly, the marine samples show the greatest spread in spectral features with the coral spectrum most strongly resembling that of the sodium bromide suggesting the biological matrix of this species is less complicated than that of the mammalian samples.

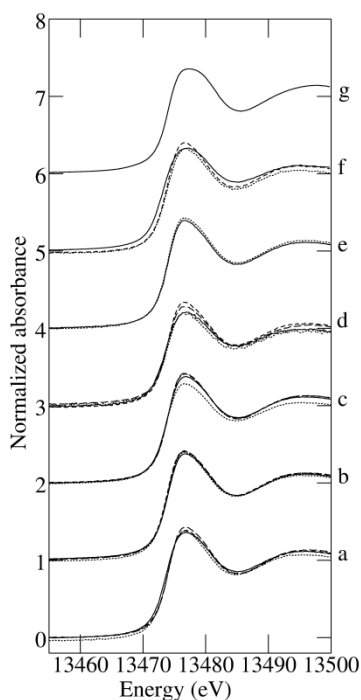


Figure 4: Br K-edge X-ray absorption near edge spectra of five different species' ovary (solid), liver (dotted), blood (dashed; solid for human) and serum samples (long dashed; dotted for human), and three marine species (solid for coral; dotted for kingfish; dashed for salmon) beneath the most closely-matching standard, sodium bromide. a) bovine, b) porcine, c) ovine, d) murine, e) human (only blood and serum spectra collected), f) marine, and g) sodium bromide.

The majority of non-ovarian spectra were fitted with $\text{NaBr}_{(\text{aq})}$ alone but the residual for TBBPA from target analysis was sufficiently low to include it in the linear combination fitting. Significant structure was evident in the residual plots (red trace in Fig. 5), with high residual values ($> 1 \times 10^{-3}$) indicating a poor fit and an incomplete representation of the bromine speciation. The result of the linear combination fitting of the $\text{Br}_{(\text{aq})}^-$ and TBBPA model compounds to the XANES spectrum of the bovine ovary is shown in Figure 5.

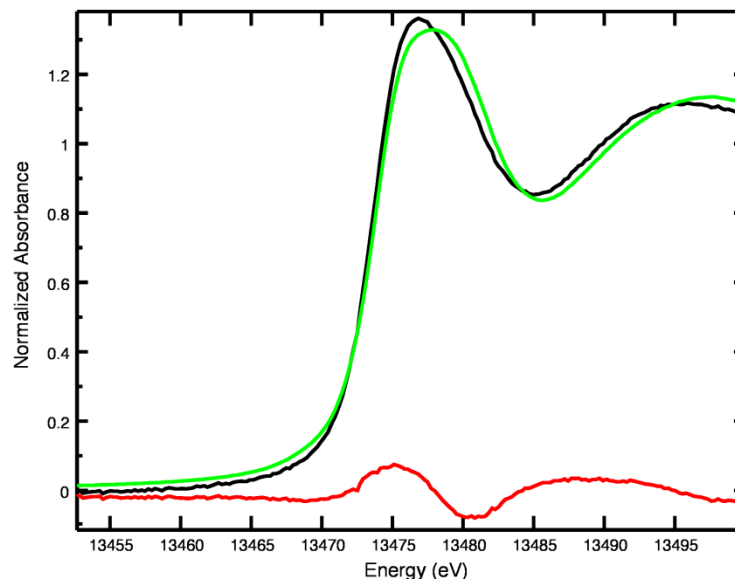


Figure 5: Comparison of Br K-edge XANES spectrum of bovine ovary tissue (black trace) against the best linear combination fit of Br model compound spectra (green trace). The percentage of the $\text{NaBr}_{(\text{aq})}$ model compound fitted was 89(2)* and that of TBBPA was 12(2)*. The residual is shown in red.

The possibility of a TBBPA-resembling compound in the ovaries of the mammalian species was concerning given that TBBPA's structure is similar to that of the thyroid hormone thyroxine (T4), except that the iodine atoms have been replaced by bromine atoms. This halogenated derivative of bisphenol A is widely used throughout the world as a flame retardant for building materials, paints, synthetic textiles, and plastic products.⁴⁰ It is a persistent and lipophilic substance which has been shown to bioaccumulate, suggesting that environmental exposure is to blame for its presence in our experimental animals.⁴¹ Although the TBBPA model compound contributed no greater than 12% to the bromine XANES spectra for bovine, ovine and porcine ovaries; based on previous quantitative experiments (ICP-MS and XRF imaging) that still suggested an extremely high concentration of 2 – 3 ppm.

In order to confirm this finding, LC-MS/MS was performed on bovine ovary tissue extracts. Despite the quantification limit for analysis being ≈ 0.25 ng/g wet mass for TBBPA, no TBBPA was detected in the extracted bovine ovaries. This finding suggests the identification of the TBBPA component by XANES fitting in samples was spurious (results presented in Supplementary Material). Thus, although the XANES fit error was reduced by the addition of the TBBPA model compound, the visual quality of the residual did not improve markedly and supplementary analysis provided no evidence for this compound being present in samples. The discrepancy between the model spectra compared with the sample spectra is then presumably due to the fact our simplified model compound of $\text{Br}^-_{(\text{aq})}$ dissolved in water did not accurately represent the *in vivo* environment for $\text{Br}^-_{(\text{aq})}$.

Principal component analysis of XANES spectra

Given the apparent similarity of the XANES spectra of all mammalian tissues and fluid samples, a PCA was performed on the spectra of the set of samples across the energy range 13.46 – 13.49 keV. The scores plot of PC2 versus PC1 (Fig. 6) clearly indicates that all samples lie in the same quadrant as the standard (NaBr), with the only deviations from the cluster appearing in the form of the four murine samples. The separation of the murine samples is most likely attributable to the extremely low concentrations of bromine present in the murine tissue and fluids and the subsequent PC differences likely arise from spectral noise, as opposed to any variation in chemical form. Given that these were laboratory reared mice their environmental exposure to Br would have been significantly less than that experienced by the other mammals, and their feed is also likely to have been of higher purity than that ingested by the other species.

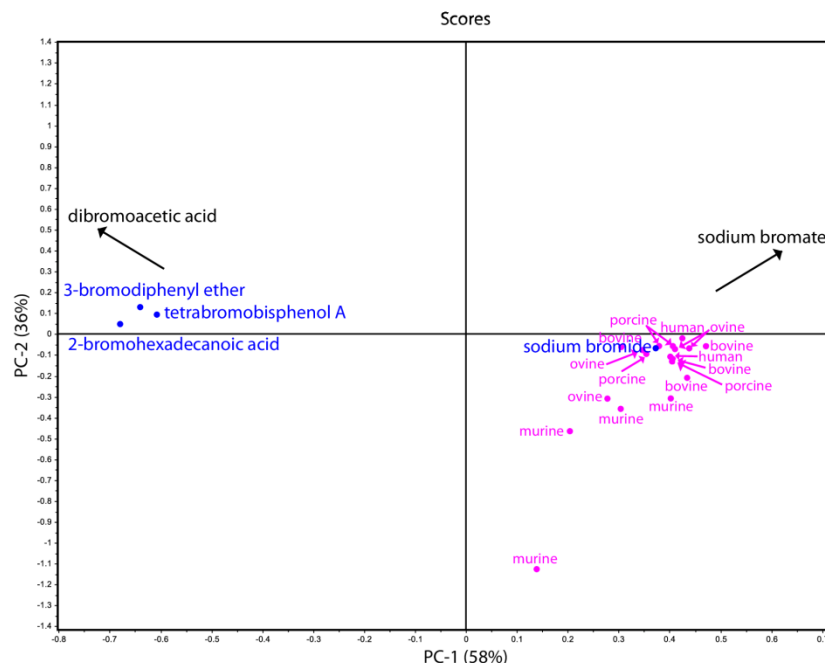


Figure 6: Scores plot of PC2 versus PC1 depicting all mammalian tissue and fluid samples (pink) clustered together with six of the Br standards (blue) predominantly separated along PC1. NaBr can be visualised as a circled point amidst the cluster of mammalian samples. For clarity bromoacetonitrile, tralomethrin, bromodichloromethane, bromochloroacetic acid, and decabromodiphenyl ether are not shown, but lie further to the left along PC1.

Conclusions

XRF imaging of bovine ovaries uncovered a widespread and consistent distribution of bromine throughout ovarian sections from 45 cows at a surprisingly high concentration. ICP-MS analysis of bovine follicular fluid and aortic serum, as well as human whole blood and serum verified this presence of bromine and suggested elemental concentrations in the same order of magnitude as the XRF analysis. Bromine K-edge X-ray absorption spectra were collected for a variety of mammalian tissue and fluids from different species (bovine, ovine, porcine, murine and human), and marine samples. Qualitative observation of the XANES region of the spectra coupled with PCA of all XAS data over the energy range 13.46 – 13.49 keV led to the conclusion that the predominant form of bromine evident in all biological samples analysed was $\text{Br}^-_{(\text{aq})}$. Biotransformation of ingested $\text{Br}^-_{(\text{aq})}$, which may have suggested a biological role, was not apparent. However, the fact that the distribution of bromine in the bovine ovaries was not completely correlated with either the X-ray thickness of the tissue or the distribution of other abundant elements suggests that the distribution of bromine, as bromide, is under some form of biochemical control.

Acknowledgements

The authors wish to acknowledge: T&R Pastoral (Murray Bridge, SA, Australia) for their donation of bovine and ovine organs and blood; Menzel's Meats Pty Ltd. (Kapanda, SA, Australia) for their donation of porcine organs and blood; David Kennaway for his donation of post mortem murine organs and blood; the technical support of Claire Wright and Jun Du in the ICP-MS and LC-MS/MS analysis of the bovine tissue samples, respectively; James Swift for his collection and initial processing of the human blood samples; Claire Weekley for her support during the XFM beamline experiments and assistance with XANES data analysis; the XFM and XAS beamline teams including David Paterson, Martin de Jonge, Daryl Howard, Simon James, Kathryn Spiers, Peter Kappen, and Chris Glover for the research that was undertaken on these beamlines at the Australian Synchrotron, Victoria, Australia; Chris Ryan for his technical support with GeoPIXE data processing; and the Australian Research Council (DP0985807, DP0984722, DP140100176) and the National Health and Medical Research Council of Australia for funding.

References

^a School of Chemistry and Physics, The University of Adelaide, SA, 5005, Australia. Fax: +61 8 8313 4380 Tel: +61 8 8313 5060; E-mail: hugh.harris@adelaide.edu.au

^b Research Centre for Reproductive Health, Discipline of Obstetrics and Gynaecology, School of Paediatrics and Reproductive Health, Robinson Research Institute, The University of Adelaide, SA, 5005, Australia. Fax: +61 8 8313 6387; Tel: +61 8 8313 3932 ; E-mail: ray.rodgers@adelaide.edu.au

^c Australian Synchrotron, Clayton, VIC, 3168, Australia. Tel: +61 3 8540 4204; E-mail: Simon.James@synchrotron.org.au

^d CSIRO Land and Water, Contaminant Chemistry and Ecotoxicology Program, Waite Campus, Adelaide, SA, 5064, Australia. Tel: +61 8 8303 8478; E-mail: Jason.Kirby@csiro.au

† Electronic Supplementary Information (ESI) available: Representative X-ray fluorescence integrated spectrum and Compton scatter maps; LC-MS/MS experimental and results.. See DOI: 10.1039/b000000x/

1. E. J. Underwood, ed., *Trace elements in human and animal nutrition*, Academic Press, Inc, New York, 1977.
2. A. S. McCall, Christopher F. Cummings, G. Bhave, R. Vanacore, A. Page-McCaw and Billy G. Hudson, *Cell*, 2014, **157**, 1380-1392.
3. F. H. Nielsen, *Journal of Trace Elements in Experimental Medicine*, 1998, **11**, 251-274.
4. R. M. Leach, Jr. and M. C. Nesheim, *J Nutr*, 1963, **81**, 193-199.
5. M. Anke, A. Regius, B. Groppe and W. Arnhold, *Acta Agronomica Hungarica*, 1990, **39**, 297-304.
6. A. A. Zhavoronkov, L. V. Kakturskii, M. Anke, B. Groppe and L. M. Mikhaleva, *Arkhiv Patologii*, 1996, **58**, 62-67.
7. S. Hellerstein, C. Kaiser, D. D. Darrow and D. C. Darrow, *Journal of Clinical Investigation*, 1960, **39**, 282-287.
8. S. Pavelka, A. Babický, M. Vobecký and J. Lener, *Industrial Toxicology '99*, 1999, 224-228.
9. M. Vobecký, A. Babický, S. Pavelka and J. Lener, *Journal of Trace and Microprobe Techniques*, 2000, **18**, 467-473.
10. C. L. Hawkins, B. E. Brown and M. J. Davies, *Archives of Biochemistry and Biophysics*, 2001, **395**, 137-145.
11. E. L. Thomas, P. M. Bozeman, M. M. Jefferson and C. C. King, *Journal of Biological Chemistry*, 1995, **270**, 2906-2913.
12. D. I. Pattison and M. J. Davies, *Biochemistry*, 2004, **43**, 4799-4809.
13. C. L. Hawkins and M. J. Davies, *Free Radical Biology and Medicine*, 2005, **39**, 900-912.
14. O. Skaff, D. I. Pattison and M. J. Davies, *Chemical Research in Toxicology*, 2007, **20**, 1980-1988.
15. G. C. Justino, M. Rodrigues, M. H. Florencio and L. Mira, *Journal of Mass Spectrometry*, 2009, **44**, 1459-1468.
16. J. Marcinkiewicz, M. Mak, M. Bobek, R. Biedron, A. Bialecka, M. Koprowski, E. Kontny and W. Maslinski, *Inflammation Research*, 2005, **54**, 42-49.
17. J. Maines, N. R. Khurana, K. Roman, D. Knaup and M. Ahmad, *Journal of Endodontics*, 2006, **32**, 886-889.
18. S. Pavelka, *Physiol. Res.*, 2004, **53**, S81-S90.
19. M. Flury and A. Papritz, *J. Environ. Qual.*, 1993, **22**, 747-758.
20. A. Kabata and H. Pendias, *New York. CRC*, 2001.
21. G. Rice, L. K. Teuschler, T. F. Speth, S. D. Richardson, R. J. Miltner, K. M. Schenck, C. Gennings, E. S. Hunter, III, M. G. Narotsky and J. E. Simmons, *Journal of Toxicology and Environmental Health-Part a-Current Issues*, 2008, **71**, 1222-1234.
22. R. Butler, A. Godley, L. Lytton and E. Cartmell, *Crit. Rev. Environ. Sci. Technol.*, 2005, **35**, 193-217.
23. P. O. Darnerud, G. S. Eriksen, T. Johannesson, P. B. Larsen and M. Viluksela, *Environ. Health Perspect.*, 2001, **109**, 49-68.
24. K. Ji, K. Choi, J. P. Giesy, J. Musarrat and S. Takeda, *Environ. Sci. Technol.*, 2011, **45**, 5003-5008.
25. D. Shanmuganathan, M. Megharaj, Z. L. Chen and R. Naidu, *Mar. Pollut. Bull.*, 2011, **63**, 154-159.
26. L. B. Owens, R. W. Vankeuren and W. M. Edwards, *J. Environ. Qual.*, 1985, **14**, 543-548.
27. F. X. R. Vanleeuwen, E. M. Dentonkelaar and M. J. Vanlogten, *Food and Chemical Toxicology*, 1983, **21**, 383-389.
28. J. G. Loeber, M. A. M. Franken and F. X. R. Vanleeuwen, *Food and Chemical Toxicology*, 1983, **21**, 391-404.
29. D. N. R. Veeramachaneni, J. S. Palmer and G. R. Klinefelter, *Journal of Andrology*, 2007, **28**, 565-577.
30. R. E. Linder, G. R. Klinefelter, L. F. Strader, M. G. Narotsky, J. D. Suarez, N. L. Roberts and S. D. Perreault, *Fundamental and Applied Toxicology*, 1995, **28**, 9-17.
31. G. R. Klinefelter, L. F. Strader, J. D. Suarez, N. L. Roberts, J. M. Goldman and A. S. Murr, *Toxicol. Sci.*, 2004, **81**, 419-429.
32. C. M. Weekley, J. B. Aitken, S. Vogt, L. A. Finney, D. J. Paterson, M. D. de Jonge, D. L. Howard, I. F. Musgrave and H. H. Harris, *Biochemistry*, 2011, **50**, 1641-1650.
33. M. C. Feiters, F. C. Kupper and W. Meyer-Klaucke, *J. Synchrotr. Radiat.*, 2005, **12**, 85-93.
34. A. C. Leri and S. C. B. Myneni, *Geochim. Cosmochim. Acta*, 2012, **77**, 1-10.
35. C. G. Ryan, *International Journal of Imaging Systems and Technology*, 2000, **11**, 219-230.
36. C. G. Ryan, *Nuclear Instruments and Methods in Physics Research Section B: Beam Interactions with Materials and Atoms*, 2001, **181**, 170-179.
37. B. Johnson-Restrepo, D. H. Adams and K. Kannan, *Chemosphere*, 2008, **70**, 1935-1944.

- 1
2
3
4
5
6
7
8
9
10
11
12
13
14
15
16
17
18
19
20
21
22
23
24
25
26
27
28
29
30
31
32
33
34
35
36
37
38
39
40
41
42
43
44
45
46
47
48
49
50
51
52
53
54
55
56
57
58
59
60
38. H. F. Rodgers, C. M. Irvine, I. L. van Wezel, T. C. Lavranos, M. R. Luck, Y. Sado, Y. Ninomiya and R. J. Rodgers, *Biology of Reproduction*, 1998, **59**, 1334-1341.
39. H. F. Irving-Rodgers, K. Hummitzsch, L. S. Murdiyarsa, W. M. Bonner, Y. Sado, Y. Ninomiya, J. R. Couchman, L. M. Sorokin and R. J. Rodgers, *Cell and Tissue Research*, 2010, **339**, 613-624.
40. S. Kitamura, T. Kato, M. Iida, N. Jinno, T. Suzuki, S. Ohta, N. Fujimoto, H. Hanada, K. Kashiwagi and A. Kashiwagi, *Life Sci.*, 2005, **76**, 1589-1601.
41. C. A. de Wit, *Chemosphere*, 2002, **46**, 583-624.